

# Microstructural development in cured soil-lime composites

M. ARABI, S. WILD

*Department of Civil Engineering and Building, The Polytechnic of Wales, Pontypridd, Mid-Glamorgan CF37 1DF, UK*

The bond which develops during curing between soil particles in the presence of lime and moisture is a result of the growth and the development of a newly formed cementitious phase (or phases). For the particular soil studied, appreciable reaction occurs between soil particles and lime only at elevated temperature, in a moist environment. The growth and development of the new phase is accompanied by an increase in compressive strength of the soil-lime composites. Scanning electron microscopy (SEM) studies show the phase to consist of an interlocking network of fine platelets and fibres, and although no direct determination of composition was possible, evidence from X-ray analysis and thermal analysis shows that the new phase is poorly crystalline and probably consists of a hydrate of calcium silicate or calcium aluminate.

## 1. Introduction

The use of lime in the stabilization of normally unsuitable soil, for roads, airfields, and other hard-wearing surfaces and also its use in upgrading existing material for building foundations and for building components, has been widely reported. The purpose of the present study is to achieve a better understanding of the mechanism of the soil-lime reaction and of the development of microstructure and strength in cured soil-lime composites at elevated temperature. This should lead to a wider and more effective use of the technique, particularly in areas of the world with high ambient temperatures. The physico-chemical changes in soil particles on reaction with lime, and the formation of new phases in such systems, is very complex and is not very well understood. However, there is quite clearly substantial evidence in the literature to indicate that the reaction of lime with clays and other finely divided alumino-silicates, results in the formation of calcium silicate hydrates and calcium aluminate hydrates, and that this is normally accompanied by the formation of some calcium carbonate due to the presence of atmospheric carbon dioxide. The hydrates formed are generally amorphous or poorly crystalline, although X-ray diffraction work has shown the formation of crystalline hydrate phases in some cases [1-8].

However, the characterization of these phases is normally based on very limited X-ray data and is often not well substantiated. The reactions between hydrated lime and different clays from the main groups such as kaolinite, montmorillonite and illite have been studied by a number of workers [1-7]. Investigations have also been made of the reaction of lime with other pozzolanic material such as pfa and amorphous silica [8]. Under various conditions, the formation of a whole range of poorly crystalline calcium silicate hydrate and calcium aluminate hydrate

phases has been reported [1-8]. In some cases the formation of specific calcium aluminium silicate hydrate (CASH) phases has also been observed. For examples, the initial reaction products from pure kaolinite reacted with lime in solution results in the formation of crystalline calcium aluminium silicate hydrate  $[Ca_2Al_2Si_3O_{10}(OH)_2]$  together with non-crystalline particles [2]. When burnt ( $650^\circ C$  for 2 h) kaolin is reacted with lime at  $20^\circ C$  for 400 days, CSHI and Stratling's compound ( $C_2ASH_n$ ) are observed [8]. Also the formation of hydrogarnets ( $C_3AS_nH_{6-2n}$ ) in soil-lime-water systems has been reported by Croft [4], Vail and Wet [6] and Lees *et al.* [7].

Because all of these different phases are made up from a relatively small group of elements which are common to most of them, and also certain of the elements i.e. aluminium and silicon have markedly similar characteristics, then interatomic distances will be similar within the structures of the different phases and the phases themselves will possess similar structural features. Therefore some of the major interatomic spacings will be common to a number of these structures. For example, the strongest X-ray reflection in gehlenite hydrate  $C_2ASH_8$  (0.287 nm) is also one of the strongest reflections in  $C_2AH_{13}$  (0.286 nm) and in  $C_2AH_8$  (0.286 nm). A second prominent reflection at 0.166 nm is also common to these three phases. Similarly prominent reflections at about 0.31, 0.28 and 0.183 nm are common to a number of calcium silicate hydrates such as CSHI, CSHII and tobermorite. Also many of these compounds are produced in extremely finely divided states. This results in very diffuse X-ray reflections which disappear altogether in the directions where crystallite dimensions became very small. Therefore it can be very misleading to characterize phases in these systems, solely on the basis of a small number of diffuse weak X-ray reflections.

## 2. Materials and experimental methods

### 2.1. Materials

The soil used (Red Marl) was obtained from a particular location in South Wales. X-ray powder diffraction and scanning electron microscopy were employed for identification of the soil minerals. The major components of the soil are quartz, feldspar and a member of the mica group illite. Minor components identified are chlorite and haematite. The lime used was a hydrated lime and its characteristics were based on BS 890 (1972). The soil was dried to constant weight at 100°C to remove any free moisture prior to mixing with lime.

### 2.2. Experimental methods

Specimens of soil–lime containing various concentrations of lime (2, 6, 10 and 14%) were mixed with “fixed” quantities of water and were compacted into cylinders (100 mm long, 50 mm diameter) of a constant density. All the specimens were prepared to BS 1924 (1975) specifications and were cured in a moist environment at various temperatures (25, 50 and 75°C) and for different times (3, 6, 12 and 24 weeks). The moist environment was maintained by wrapping the specimens in two layers of cling-film and sealing in polythene boxes. For the long curing times any water loss was made up by holding the specimens in moist sand at periodic intervals until their original weight was achieved and then continuing with the curing process. Thus the original moisture content of the specimens was maintained constant during the curing process. Initially three and sometimes four specimens were made up for each test. However, in view of the consistency of the results achieved for these initial specimens the number of specimens was reduced to two per test throughout the work. After measuring

unconfined compressive strength, samples were taken for SEM investigations, X-ray analysis and thermogravimetric analysis. A Cambridge S 150 SEM was employed for the microstructural investigations. Fragments of the specimens were taken and the free water in the samples was removed by vacuum drying. The samples were covered with a thin layer of evaporated gold and the fracture surface was examined in the SEM. X-ray diffraction analysis was carried out using a Hägg–Guinier focusing camera employing monochromatic  $\text{CrK}\alpha$  radiation, and a Perkin–Elmer thermal analyser (model TGS-2) was employed for the thermogravimetric analysis.

About 10 to 11 mg of finely powdered sample was used for thermogravimetric analysis. To ensure reproducibility of the sampling technique and to check that each sample was representative of the whole, a number of samples were taken from the same batch in the initial stages. Subsequently periodic checks were made for consistency during the thermogravimetric work. The heating rate was  $20^\circ\text{C min}^{-1}$  and the sensitivity used for the DTG was  $0.1\text{ mg min}^{-1}$ . All tests were carried out in a dry,  $\text{CO}_2$  free, nitrogen atmosphere.

## 3. Results

### 3.1. Soil analysis

X-ray powder diffraction data are given in Table I and TG and DTG traces of the soil are presented in Fig. 1. Fig. 2 shows a scanning electron micrograph of the soil particles. It can be seen in Table I, that the soil consists of illite, together with quartz, feldspar, chlorite and haematite. The DTG results are characteristic of illite (see [10, 11]) which shows two main distinctive features. These are: (a) a medium-sized low temperature peak at 100 to 150°C; and (b) a medium-sized dehydroxylation peak at about 550 to 600°C, which is very broad, beginning at about 400°C and continuing up to about 900°C.

These peaks are clearly visible in Fig. 1.

Scanning electron micrographs of the soil particles show that a large proportion of the soil consists of plate-like particles of typical illite morphology (see [12, 13]). As the X-ray and thermogravimetric results show illite to be a major component of the clay

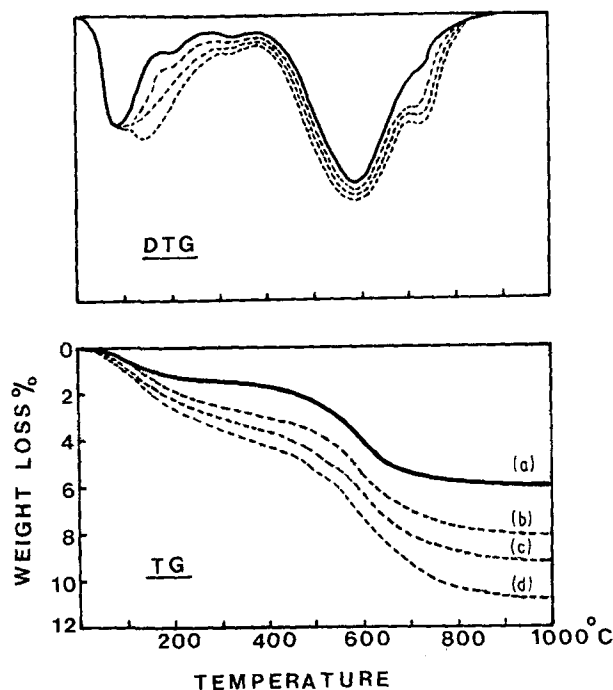


Figure 1 Thermogravimetric results for soil and cured soil–lime samples, cured for 24 weeks at 50°C. (a) soil, (b) soil and 6 wt % lime; (c) soil and 10 wt % lime; (d) soil and 14 wt % lime.

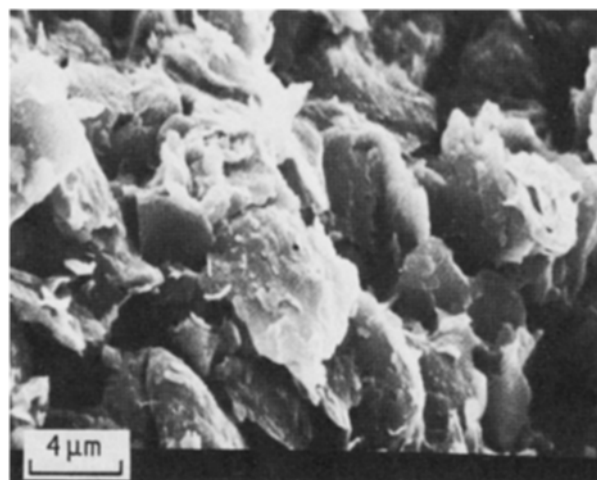


Figure 2 Scanning electron micrograph of the soil,  $\times 3500$ .

fraction of the soil, these plate-like particles are considered to consist predominantly of illite.

### 3.2. Analysis of cured samples

Fig. 3 shows the variation in unconfined compressive strength with lime content for the 24 week cured samples. Clearly strength development is negligible at ambient temperatures but increases rapidly with increasing temperature. Table II gives mass balance data obtained from TG traces for soil–lime samples containing 2, 6, 10 and 14 wt % lime, cured in a moist environment for various times (3, 8, 12 and 24 weeks) at 50°C.

The results show that the initial free lime is gradually used up as the curing time is increased. This is apparent from a general decrease with curing time in the observed weight loss corresponding to the dehydroxylation of calcium hydroxide at about 400 to 550°C (see column H).

Thermogravimetric analysis of the initial lime itself showed the expected large dehydroxylation peak at 480°C together with a very small peak at 750°C resulting from carbonate contamination. This was accounted for in the mass balance calculations (see column K). As the amount of lime used up during curing increases, there is a corresponding increase in two additionally observed weight losses on TG and DTG traces at 100 to 250°C (column E) and at 650 to 800°C (column L). This is clearly shown in the examples of Fig. 1. The former of these is equivalent to that found in the thermal analysis of calcium silicate hydrate [8, 10] and a calcium aluminate hydrate [14] and corresponds to the loss of water from the hydrates. The latter results from the decomposition of calcium carbonate, the majority of which is formed during the curing period as a result of partial carbonation of the

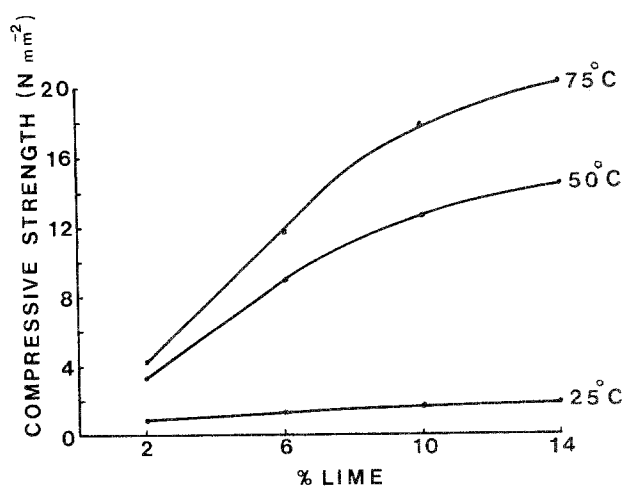


Figure 3 Variation in compressive strength with lime content for 24 week moist-cured specimens at different temperatures.

lime. The amount of carbonation occurring tends to be very erratic and although it generally increases with increasing lime content, there is no observed systematic variation with curing time. It is, however, likely that some carbonation of residual free lime occurred in the period between compression testing and thermogravimetric analysis as no special precautions were observed to prevent further carbonation in this period. A third source of carbonate contamination is in the soil itself which shows minor traces, detectable both by EDAX and DTG but not detectable by X-ray powder diffraction analysis. This was also taken into account in the mass balance calculations (column J). It was therefore possible from mass balance considerations to determine for the cured samples the proportion of lime that was unaccounted for, either as residual  $\text{Ca}(\text{OH})_2$  or  $\text{CaCO}_3$ . Clearly this lime, termed

TABLE I X-ray powder diffraction analysis of soil (Red-Marl)

| d(nm) | Intensity | Minerals   | d(nm) | Intensity | Minerals  |
|-------|-----------|------------|-------|-----------|-----------|
| 1.420 | vw        | Chl        | 0.270 | w         | Ha        |
| 0.999 | w         | Il         | 0.264 | vw        | Fel       |
| 0.707 | w         | Chl        | 0.260 | vw        | Chl       |
| 0.639 | vw        | Fel        | 0.256 | w         | Il-Fel    |
| 0.498 | vw        | Il         | 0.252 | vw        | Ha-Chl    |
| 0.472 | vw        | Chl        | 0.246 | w         | Qu-Il-Chl |
| 0.447 | m         | Il         | 0.238 | vw        | Il-Chl    |
| 0.426 | s         | Qu         | 0.232 | vw        | Qu        |
| 0.412 | vw        | Il         | 0.228 | w         | Qu        |
| 0.403 | vw        | Fel        | 0.224 | vw        | Qu-Il     |
| 0.389 | vw        | Fel        | 0.220 | vw        | Ha        |
| 0.387 | vw        | Fel-Il     | 0.219 | vw        | Il        |
| 0.376 | vw        | Fel        | 0.215 | vw        | Il        |
| 0.373 | vw        | Fel        | 0.213 | w         | Qu        |
| 0.367 | vw        | Ha-Fel     | 0.198 | w         | Qu-Il     |
| 0.352 | vw        | Fel-Chl    | 0.184 | vw        | Ha        |
| 0.334 | vs        | Qu-Il      | 0.181 | m         | Qu        |
| 0.321 | w         | Fel-Il     | 0.180 | vw        | Qu        |
| 0.318 | vw        | Fel        | 0.169 | vw        | Ha        |
| 0.317 | vw        | Fel        | 0.167 | w         | Qu        |
| 0.299 | vw        | Fel        | 0.166 | vw        | Qu        |
| 0.297 | vw        | Il         | 0.154 | m         | Qu        |
| 0.293 | vw        | Fel        | 0.150 | w         | Il        |
| 0.286 | vw        | Il-Chl-Fel | 0.145 | w         | Qu        |
| 0.279 | vw        | Il         | 0.137 | m         | Qu        |

Key: w – weak, vw – very weak, m – medium, vs – very strong Chl – chlorite, Il – illite, Fel – feldspar, Qu – quartz, and Ha – haematite.

TABLE II Mass balance calculations for cured soil-lime samples

| Curing period (week) | Percentage of lime (%) | Cured sample weight (mg) | Free water in sample (mg) | Gel water at 100 to 250°C (mg) | Original weight of soil (mg) | Original weight of lime added (mg) | Free lime in cured sample (mg) | Weight of calcium carbonate (mg) in |               |               |                             | Consumed lime (mg) | Consumed lime (%) |       |
|----------------------|------------------------|--------------------------|---------------------------|--------------------------------|------------------------------|------------------------------------|--------------------------------|-------------------------------------|---------------|---------------|-----------------------------|--------------------|-------------------|-------|
|                      |                        |                          |                           |                                |                              |                                    |                                | cured sample                        | original soil | original lime | formed during curing period |                    |                   |       |
| A                    | B                      | C                        | D                         | E                              | F                            | G                                  | H                              | I                                   | J             | K             | L                           | M                  | N                 | O     |
| 3                    | 2                      | 9.09                     | 0.14                      | 0.02                           | 8.75                         | 0.17                               | 0.04                           | 0.20                                | 0.16          | 0.01          | 0.03                        | 0.02               | 0.10              | 1.14  |
| 12                   | 2                      | 11.00                    | 0.12                      | 0.03                           | 10.62                        | 0.21                               | 0.09                           | 0.28                                | 0.19          | 0.01          | 0.08                        | 0.06               | 0.05              | 0.47  |
| 24                   | 2                      | 11.45                    | 0.14                      | 0.03                           | 11.06                        | 0.22                               | 0.00                           | 0.21                                | 0.20          | 0.01          | —                           | —                  | 0.21              | 1.90  |
| 8                    | 6                      | 10.47                    | 0.09                      | 0.05                           | 9.75                         | 0.58                               | 0.12                           | 0.21                                | 0.18          | 0.03          | —                           | —                  | 0.43              | 4.41  |
| 12                   | 6                      | 10.53                    | 0.14                      | 0.06                           | 9.72                         | 0.58                               | 0.03                           | 0.31                                | 0.18          | 0.03          | 0.10                        | 0.07               | 0.45              | 4.63  |
| 24                   | 6                      | 11.40                    | 0.12                      | 0.08                           | 10.54                        | 0.63                               | 0.02                           | 0.33                                | 0.19          | 0.03          | 0.11                        | 0.08               | 0.50              | 4.74  |
| 8                    | 10                     | 10.48                    | 0.09                      | 0.08                           | 9.34                         | 0.93                               | 0.17                           | 0.36                                | 0.17          | 0.05          | 0.14                        | 0.10               | 0.61              | 6.53  |
| 12                   | 10                     | 10.67                    | 0.05                      | 0.08                           | 9.53                         | 0.95                               | 0.14                           | 0.44                                | 0.17          | 0.05          | 0.22                        | 0.16               | 0.60              | 6.30  |
| 24                   | 10                     | 11.80                    | 0.13                      | 0.12                           | 10.47                        | 1.05                               | 0.06                           | 0.35                                | 0.19          | 0.06          | 0.10                        | 0.07               | 0.86              | 8.21  |
| 3                    | 14                     | 11.56                    | 0.12                      | 0.07                           | 9.84                         | 1.38                               | 0.28                           | 0.95                                | 0.18          | 0.08          | 0.69                        | 0.51               | 0.51              | 5.18  |
| 12                   | 14                     | 10.73                    | 0.12                      | 0.10                           | 9.11                         | 1.28                               | 0.16                           | 0.70                                | 0.17          | 0.07          | 0.46                        | 0.34               | 0.71              | 7.79  |
| 24                   | 14                     | 11.44                    | 0.14                      | 0.16                           | 9.72                         | 1.36                               | 0.09                           | 0.49                                | 0.18          | 0.08          | 0.23                        | 0.17               | 1.02              | 10.49 |

*Key of calculations*

- A Age of specimens cured at 50°C in moist environment.  
 B Initial lime concentration, expressed as a percentage of dry (100°C) soil.  
 C Cured sample weight used in thermogravimetric analysis.  
 D Free water in cured sample, determined by TG over temperature range 20 to 100°C.  
 E Gel water in cured sample, determined by TG over temperature range 100 to 250°C.  
 F Original weight of soil in cured sample, determined from  $F = [C - (D + E) - (L - M)] / (100 + B) \times 100$ .  
 G Original weight of lime in cured sample, determined from  $G = F \times B / 100$ .  
 H Free lime (unreacted) in cured sample, determined by TG over temperature range 400 to 550°C.  
 I Weight of calcium carbonate in cured sample, determined by TG over temperature range 650 to 800°C.  
 J Weight of calcium carbonate in original soil, determined by TG.  
 K Weight of calcium carbonate in original lime, determined by TG.  
 L Weight of calcium carbonate formed during the curing period, determined from  $L = I - (J + K)$ .  
 M Weight of  $\text{Ca}(\text{OH})_2$  equivalent to L.  
 N Weight of "consumed lime" in cured sample, determined from  $N = G - (H + K + M)$ .  
 O Wt% "consumed lime", expressed as a percentage of dry (100°C) soil determined from  $O = (N/F) \times 100$ .

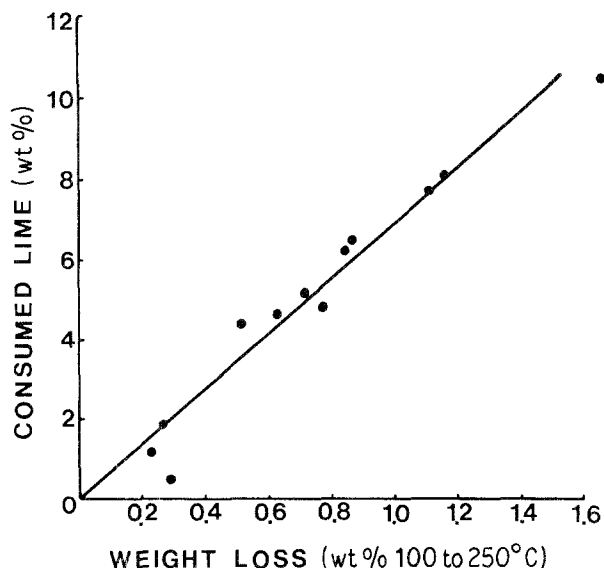


Figure 4 Plot of the wt % "consumed lime" against the wt % loss of "gel water" in the temperature region 100 to 250°C.

"consumed lime" (column O) has reacted with some component of the soil. Fig. 4 shows a plot of the wt % of "consumed lime" against the wt % loss (during TG analysis) in the temperature region 100 to 250°C. The relationship is that which would be expected if the "consumed lime" is being used up in forming cementitious calcium silicate hydrates or calcium aluminate hydrates which subsequently lose the major part of their gel water in this temperature region. Taylor [15] has shown for cement pastes that although gel water from the cementitious phases is lost over a wide range of temperature the major part of it (60%) is evolved in the temperature region 100 to 250°C. The strength of the cured samples might also be expected to be directly related to the proportion of any cementitious products in the system. Fig. 5, which shows a plot of compressive strength against the weight per cent of "consumed lime", for specimens cured at 50°C for various times, clearly supports this hypothesis. X-ray powder diffraction analysis, however, gives no strong evidence

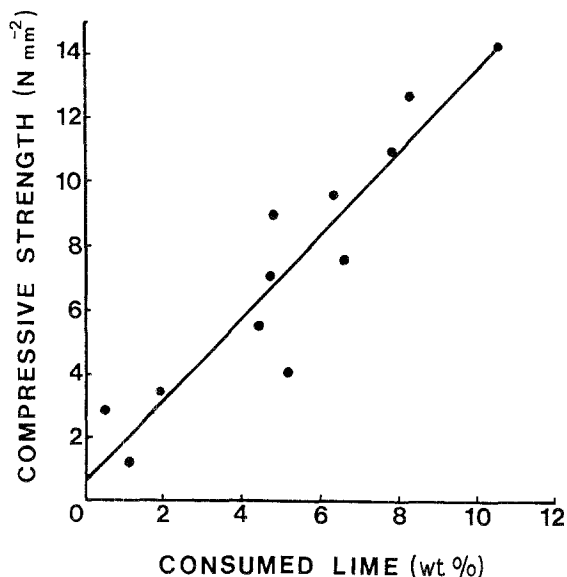


Figure 5 Plot of unconfined compressive strength against wt % "consumed lime" for soil-lime specimens cured at 50°C for various times.

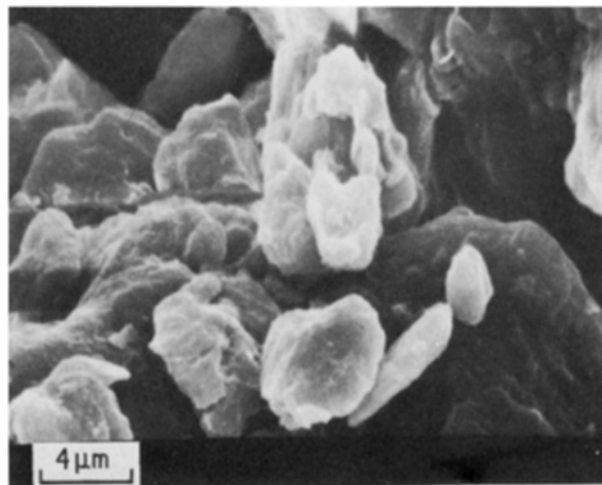


Figure 6 Scanning electron micrograph of the fracture surface of a 1 day (75°C) cured soil-10 wt % lime sample,  $\times 3500$ .

for the formation of additional crystalline reaction products. In order to promote growth and crystallization of any amorphous reaction products which may be forming, curing temperature were increased to 75°C. This resulted in the appearance in the X-ray diffraction pattern of two additional very weak diffraction peaks with  $d$  spacing of 0.307 nm, which corresponds to the strongest diffraction peak for CSH gel, and 0.303 nm which corresponds to the strongest diffraction peak for calcite. This information alone, as previously indicated, is insufficient evidence to positively confirm the formation of cementitious calcium silicate hydrate phases. However, scanning electron microscopy did produce positive evidence of the formation and growth of a new cementitious phase or phases. Fig. 6 shows the microstructure of a 1 day cured sample of soil-10 wt % lime, which when compared with the untreated soil micrograph of Fig. 2 shows very little evidence of any growth. Fig. 7, however, shows the microstructure of samples cured for 3 weeks and here, there is a marked change in morphology with clear evidence of the development of new material both at the edges and at the surface of the original soil particles. Fig. 8 shows the microstructure of this new product at a curing time of 6 weeks.

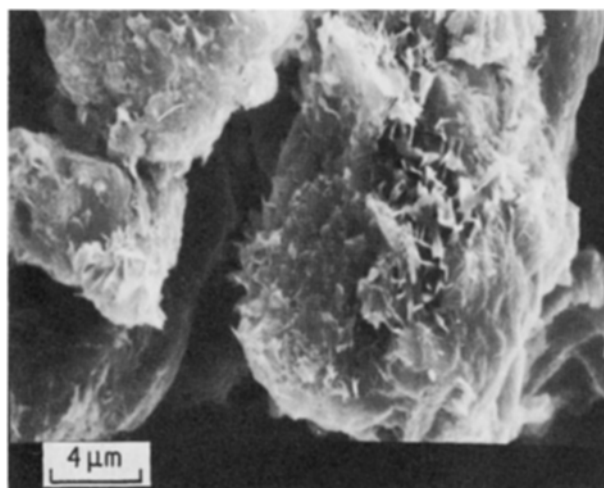


Figure 7 Scanning electron micrograph of the fracture surface of a 3 week (75°C) cured soil-10 wt % lime sample,  $\times 3500$ .

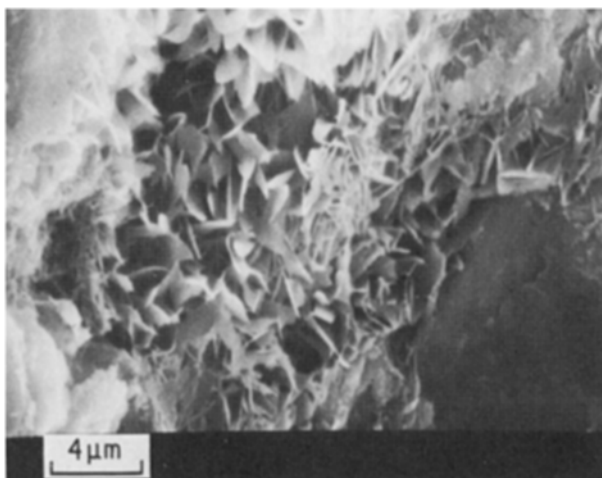


Figure 8 Scanning electron micrograph of the fracture surface of a 6 week (75°C) cured soil-10 wt % lime sample,  $\times 3500$ .

At this stage, the new phase consists of an interlocking network of fine plate-like particles. After curing for 3 weeks, there is insufficient material to form bridges between adjacent soil particles, but after curing for 6 weeks the interlocking network of plate-like particles has grown into the interstices to form a continuous network. Also by 6 weeks the plate-like particles have increased considerably in size and are 2 to 4  $\mu\text{m}$  across. For even longer curing times a much denser material is produced. Fig. 9 shows a fracture surface for a specimen cured for 12 weeks and the interlocking network of plate-like particles has now developed into a dense mat of material. The form of the microstructure is clearly analogous to that produced in hydrated cement paste (see [16, 17]). The composition of these newly formed plates is at present unknown. As mentioned above the X-ray powder diffraction results from samples cured for 24 weeks indicate no significant formation of new crystalline phases, although the SEM observations clearly depict formation of new material on a large scale which confirms that, the newly formed material is very poorly crystalline.

#### 4. Conclusions

It has been shown that the clay component (illite) of



Figure 9 Scanning electron micrograph of the fracture surface of 12 week (75°C) cured soil-10 wt % lime sample,  $\times 3500$ .

a particular soil, reacts with hydrated lime under favourable curing conditions to produce a new cementitious phase. This is confirmed by microstructural examination of fracture surfaces which show very limited evidence for the formation of a cementitious product at low temperatures but clear evidence of massive formation of cementitious product at the high curing temperature. Electron micrographs taken at an early stage of curing (1 day) show a modification in particle shape which results from initial dissolution of material. Specimens cured in moist conditions at elevated temperatures (75°C), and at various curing times (3, 6 and 12 weeks), show the formation, growth and development of this new phase. The phase grows on the surface and the edges of the illite particles. It has a very characteristic morphology consisting of a matrix of interlocking fibres and platelets. There are also marked similarities between this phase and the C-S-H phase found in cured ordinary Portland cement. The scanning electron micrographs show how this new phase develops to fill up the pores and link the soil particles together as the curing time is increased. X-ray evidence confirms that the new phase is very poorly crystalline, and, therefore complete characterization is not possible using this technique. However, thermogravimetric analysis together with measurements of compressive strength show that:

1. a proportion (termed "consumed lime") of the initial added lime is unaccounted for as either calcium carbonate or residual calcium hydroxide in cured samples;
2. there is a significant loss of water from cured samples in the temperature region 100 to 250°C. This behaviour is similar to that of cured Portland cement where gel water is lost from the C-S-H and C-A-H phases in this temperature region;
3. the weight per cent of "consumed lime" present is proportional to the weight per cent of water lost in this temperature region;
4. the compressive strength of cured soil-lime compacts is also proportional to the weight per cent of "consumed lime" present in the system.

These observations clearly indicate that, a new calcium-containing hydrate is being formed which is similar to the calcium-containing hydrates formed on hydration of Portland cement. Further work involving transmission electron microscopy and energy dispersive analysis is in progress in order to confirm this hypothesis and obtain a positive composition for this phase. Additional curing programmes are also being carried out aimed at eliminating the problems of carbonate contamination and of increasing the volume fraction of cementitious phase being formed.

#### Acknowledgements

The authors would like to thank Mr R. D. McMurray for providing the facilities within his Department for successful completion of the project, Dr R. Delpak and Mr G. O. Rowlands for helpful discussions on the work, Mrs C. Tindall and Mr B. Minty for technical assistance with SEM and XRD techniques and Dr G. J. Rees for assistance with thermal analysis.

## References

1. J. L. EADES and R. E. GRIM, *Highway Research Board Bulletin* **262** (1960).
2. R. L. SLOAN, "Early reaction in the Kaolinite-hydrated lime-water system", in Proceedings of the 6th International Conference on Soil Mechanics and Foundation Engineering, Montreal, Vol. 1 (1965) pp. 121-5.
3. S. DIAMOND, J. L. WHITE and W. L. DOLCH, "Transformation of Clay Minerals by Calcium Hydroxide Attack", Proceedings, 12th National Conference on Clays and Clay Minerals edited by W. F. Bradley (Pergamon Press, New York, 1964) pp. 359-79.
4. J. B. CROFT, "The processes involved in the lime-stabilization of clay soils", Proceedings, Australian Road Research Board, Sydney, Vol. 2, part 2 (1964) pp. 1169-200.
5. A. LE ROUSE, "Trailements des sols argileux par la chaux", Bull. Liaison Laho, Routiers P. et Ch. No. 40 (1969) pp. 59-96.
6. J. W. VAIL and J. D. WET, *J. Amer. Ceram. Soc.*, **55** (1972) 432.
7. G. LEES, M. D. ABDELKADER, and S. K. HAMDANI, *J. Inst. Highways and Transportation* **30** (12) (1983) 8.
8. J. JAMBOR, *Mag. Concr. Res.* **15** (45) (1963) 131.
9. Transportation and Road Research Board, "State of the art; Lime stabilization", Transportation Research Circular, No. 180 (1976) pp. 1-31.
10. R. C. MACKENZIE, "Differential Thermal Analysis", Vol. 1 (Academic Press, London, 1970) pp. 517, and 592.
11. R. E. GRIM, "Applied Clay Mineralogy" (McGraw Hill, New York, 1960) p. 102.
12. H. BEUTELSPACHER and H. W. VANDER MARCEL, "Atlas of electron microscopy of clay minerals and their admixtures" (Elsevier, Amsterdam, 1967) pp. 117-18, 127-9.
13. R. N. YONG and B. P. WARKENTIN, "Soil properties and behaviour" (Elsevier, Amsterdam, 1975) p. 81.
14. F. M. LEA, "The Chemistry of Cement and Concrete" (Edward Arnold, London, 1976) p. 207.
15. H. F. W. TAYLOR, "Studies on the Chemistry and Microstructure of Cement Pastes", Proceedings of the Conference on Chemistry and Chemically Related Properties of Cement, Imperial College, April 1984 (The British Ceramic Society, London, 1984) pp. 65-82.
16. S. DIAMOND, "Cement Paste Microstructure", Proceedings of the Conference on Hydraulic Cement Pastes—Their Structure and Properties, Sheffield, 1976 (Cement and Concrete Association, Slough, 1976) p. 2.
17. B. J. DALGLEISH and P. L. PRATT, *J. Mater. Sci.* **17** (1982) 2199.

*Received 22 February  
and accepted 20 March 1985*